Supported Dense Ceramic Membranes for Oxygen Separation

Final Report

Period Starting: June 25, 1998
Period Ending: June 26, 2002

The Annual Technical Report for the report period June 25, 2001 to June 26, 2002 is incorporated within

Timothy L. Ward

July 2002

DOE Award No.: DE-AC26-98FT40120

University of New Mexico
Department of Chemical and Nuclear Engineering
Albuquerque, NM 87131

DISCLAIMER

ABSTRACT

Mixed-conducting ceramics have the ability to conduct oxygen with perfect selectivity at elevated temperatures, making them extremely attractive as membrane materials for oxygen separation and membrane reactor applications. While the conductivity of these materials can be quite high at elevated temperatures (typically 800-1000 °C), much higher oxygen fluxes, or, alternatively, equivalent fluxes at lower temperatures, could be provided by supported thin or thick film membrane layers. Based on that motivation, the objective of this project was to explore the use of ultrafine aerosol-derived powder of a mixed-conducting ceramic material for fabrication of supported thick-film dense membranes. The project focused on the mixed-conducting ceramic composition $SrCo_{0.5}FeO_x$ (SCFO) because of the desirable permeability and stability of that material, as reported in the literature. Appropriate conditions to produce the submicron $SrCo_{0.5}FeO_x$ powder using aerosol pyrolysis were determined. Porous supports of the same composition were produced by partial sintering of a commercially obtained powder that possessed significantly larger particle size than the aerosol-derived powder. The effects of sintering conditions (temperature, atmosphere) on the porosity and microstructure of the porous discs were studied, and a standard support fabrication procedure was adopted. Subsequently, a variety of paste and slurry formulations were explored utilizing the aerosol-derived SCFO powder. These formulations were applied to the porous SCFO support by a doctor blade or spin coating procedure. Sintering of the supported membrane layer was then conducted, and additional layers were deposited and sintered in some cases. The primary characterization methods were X-ray diffraction and scanning electron microscopy, and room-temperature nitrogen permeation was used to assess defect status of the membranes.

We found that non-aqueous paste/slurry formulations incorporating dispersant, plasticizer and binder provided superior cracking resistance compared to simple water, alcohol, or polyethylene glycol (PEG) based formulations. With a formulation employing castor oil as dispersant, isopropyl alcohol/mineral spirits as solvent, polyvinyl butyral as binder, and dibutyl phthalate/PEG as plasticizer, sintered SCFO membrane layers approximately 5 μm thick with no apparent cracks were prepared using spin coating with several coats and sintering cycles. A similar but more viscous formulation applied by doctor blade gave a ~10 μm thick membrane layer in one coat, but with some apparent cracking. We demonstrated that the membrane layer could be densified while retaining porosity in the chemically identical support. This was accomplished by pre-sintering the support in air (1050 °C), which coarsened the grain size and provided a relatively stable plate-shaped granular microstructure, followed by membrane layer fabrication with the highly-sinterable aerosol powder. Final densification was conducted by sintering in nitrogen (~1100 °C), which provided accelerated sintering rates and led to the desired layered perovskite phase content. In spite of these successes, low-temperature pressure-driven permeation testing with N_2 showed that even the best membranes were not sufficiently defect free for high-temperature oxygen permeation testing. The source of these defects were not readily apparent from scanning electron microscopy, though incomplete or nonuniform membrane layer coverage from edge to edge of the support was probably one important factor.

TABLE OF CONTENTS

EXECUTIVE SUMMARY

Ceramic mixed-conducting membranes separate oxygen with perfect selectivity via ionic oxygen transport by vacancy or interstitial diffusion through the crystalline material.[1-11] The potential impact of such membranes for high-temperature applications such as partial oxidation reactors and oxidative reformers is well recognized.[1-4] The performance of several compositions of this type of membrane has been demonstrated using thick-walled ceramic membranes (wall thickness of 0.5 - 1.0 mm).[4-10] There is a drive to develop reliable methods to fabricate thin or thick film membranes so that solid-state diffusional resistance can be minimized, and oxygen flux thus maximized. Reliable fabrication of dense ceramic membrane films on porous supports has been a challenging task that has still not been solved, though there have been some instances of reported success. These issues provided the motivation for this project.

The overall objective of this project was to explore important fundamental and practical issues confronting the successful development of thick-film dense ceramic membrane technology for oxygen separation. More specifically, the project goals were to: utilize aerosol pyrolysis[12,13] to produce ultrafine powders for fabrication of thick film Sr-Co-Fe-O (SCFO) membranes, explore strategies for fabrication of defect-free thick-film membranes on porous supports using those powders, develop an improved understanding of the fundamental issues impacting successful thick film membrane fabrication (such as particle deposition and infiltration into porous supports, film and support sintering behavior, crystalline phase evolution, and membrane stability), and explore and demonstrate the use of a novel metal organic chemical vapor deposition technique to mend membrane defects.

The fabrication strategy in this project was to deposit thin or thick films of ultrafine powders produced by aerosol pyrolysis[12,13] onto (or into) partially sintered porous supports, followed by co-sintering of the film and support, with the objective of densifying the film while retaining open porosity in the support. The porous supports were made using a commercially-obtained $SrCo_{0.5}FeO_x$ powder possessing relatively large (~10 μm) particle agglomerates. The same overall composition was used for the dense membrane layer, prepared from aerosol-derived powder. The $SrCo_{0.5}FeO_x$ composition was chosen because it has been reported to have a high oxygen permeability, while also possessing good phase stability in reducing environments that are typical of important applications involving synthesis gas (CO/H_2).[4,9-11]

The research conducted during this project can be divided into four major areas: (1) support fabrication, (2) membrane powder synthesis, (3) powder paste/slurry formulation and deposition, and (4) supported membrane sintering. Relatively early in the project, the sintering behavior of the supports in different atmospheres was studied, leading to the following standard support fabrication procedure. Commercial $SrCo_{0.5}FeO_x$ powder was uniaxially pressed at 64 MPa, followed by sintering in air at 1050 °C (ramp rate 5 °C/min with 2 hr soak) to give supports with typical thickness of 1.5 mm, diameter 13.4 mm, and approximately 50% porosity. After air sintering, X-ray diffraction (XRD) data were indexed well to the compound $Sr_7Fe_{10}O_{22}$ in the JCPDS data base. The literature indicates that this phase is probably isostructural with $Sr_4Fe_{6-x}Co_xO_{13}$,[14,15] a phase that has a perovskite intergrowth structure that develops platelet-shaped grains. This is consistent with our observations that air sintering led to plate-shaped grains that are relatively difficult to sinter to high density; whereas nitrogen sintering led to more equiaxed grains, much more rapid sintering, and phase content that included CoO and a brownmillerite

phase. Air sintering was chosen for the supports largely because it provided a support that was less active for further sintering in subsequent membrane deposition and sintering steps.

Appropriate synthesis conditions for production of submicron $SrCo_{0.5}FeO_x$ by aerosol pyrolysis were also established early in the project. After exploring various reactor temperatures and atmospheres, a standard powder synthesis procedure was adopted that utilized air as the carrier gas and a reactor temperature of 700 °C. The powder possessed a mean particle size of approximately 0.3 μm, and consisted of essentially single-phase cubic perovskite. This was an attractive precursor powder for membrane deposition and further processing to ultimately produce a dense layer of the layered perovskite phase.

The most involved and challenging aspect of this project was exploring paste and slurry formulations, along with deposition methods and sintering procedures, for producing defect and crack-free membrane layers. Our earliest approach utilized dilute aqueous slurries, and we later investigated in some depth the use of doctor blade deposition of thicker pastes prepared using 400 MW polyethylene glycol (PEG). These pastes, that were typically ~20 wt% aerosol-derived powder, yielded individual layers of 20-30 μm thickness prior to sintering, providing sintered membranes of 5-10 μm thickness. The particle layer before sintering was continuous, uncracked and highly porous. Relatively little densification of the film occurred below 800 °C, however rapid sintering occurred above 900 ^{o}C, accompanied by cracking or opening up of the film. In air, plate-shaped grains developed, which retained significant open porosity (apparent by SEM) to temperatures above 1150 ^{o}C, whereas nitrogen sintering retains approximately equiaxed particle structure leading to elimination of porosity in the film at approximately 1050 ^{o}C. The observed microstructures of the films were consistent with those seen in sintering studies of the porous supports. The films, which started as the SCFO perovskite phase prior to sintering (i.e. as-produced SCFO powder), evolved into a composite mixture of layered perovskite and CoO after sintering in N_2 at 1050 ^{o}C. This phase mixture is consistent with literature reports for successful thick-wall membranes of this composition.[10,11]

This paste formulation and deposition procedure allowed us to demonstrate control of the membrane phase and densification of the membrane layer without simultaneous densification of the support, both important milestones for the project. Unfortunately, the conditions that lead to a high degree of film densification also caused development of large cracks and open areas in the film as shrinkage occurs in the film. Two approaches were explored to address the issue of cracking in the membrane layer. One strategy involved utilizing a composite formulation for the support so that sintering temperatures very near partial melting could be employed to densify the membrane layer. The reasoning was that under such conditions, sufficient stress would not develop in the film to cause cracking. Utilizing MgO mixed with $SrCo_{0.5}FeO_x$ for the porous support, we showed that sintering temperature of 1300 to 1400 °C could be employed with densification of the support. Under these sintering conditions, cracking in the membrane layer was averted; however, the films retained a porous open structure with sintering for reasons that were never fully understood.

The second approach to alleviate membrane cracking involved exploring non-aqueous paste and slurry formulations containing binder, dispersant and plasticizer components. We also explored spin coating as an alternative to the doctor blade procedure reported earlier. The spin-coating

procedure led to much more uniform coverage over the porous substrate, but required the paste formulation to be modified to provide lower viscosity. The components and approximate proportions of the paste/slurry formulas were identified from ceramic tape casting formulations found in the literature.[16] The solvent used was mineral spirits and isopropanol in a 2:1 ratio (by weight). To this, castor oil was added as a dispersant (0.083 g/g solvent), polyvinyl butyral as a binder (0.125 g/g solvent), and dibutyl phthalate, polyethylene glycol (MW 300) and stearic acid as plasticizers (each 0.083/g solvent). The final paste/slurry formulations consisted of this mixture, powder, and additional solvent and/or castor oil in some cases.

The formulation of pastes for doctor blade application were improved by using 25-30 wt% castor oil (in excess of what was present in the solvent mixture), allowing pastes with up to 40 wt% powder to be prepared. Films prepared from these pastes sintered to apparently complete density (by SEM examination) at 1100 °C in N_2, while leaving the support porous. Cracking was much improved, but still existed. We found that the doctor blade technique did not give good control over thickness, uniformity, or edge-to-edge coverage. Since complete film coverage is critical for permeation testing, we explored spin coating as an alternative. A modified slurry formulation was developed which utilized extra solvent, with the powder content reduced to 15-18 wt%. Layer-by-layer sequential depositions were done with sintering and characterization after each layer. We found that the first membrane layer was very thin with apparent open porosity, but that membranes of two or more layers had essentially complete edge-to-edge coverage of the substrate, with no apparent cracks or prominent defects by SEM. Room temperature N_2 leak testing on a 4-coat membrane (thickness ~6 μm) revealed a permeability about 5-6 times lower than the original support, and the 2-coat and 3-coat membrane layers were comparable. These were the highest quality and most promising membranes produced in the project. The membrane deposition methodology utilizing organic-based pastes was a substantial improvement over previous methodologies. However, we were still unable to reduce leakage levels to a sufficiently low level for practical O_2 permeation testing or service.

The use of non-aqueous slurry formulations led to dramatic improvements of film microstructure, with essentially complete elimination of cracking. In addition, the strategy of using deposition of multiple thin layers, each with roughly micron thickness, was significantly more successful that the deposition of single thick layers with thickness of more than 10 microns. Our inability to produce sufficiently defect-free membranes for high temperature permeation testing appears to have been related to the following factors: imperfect edge-to-edge uniformity in the membrane layer, and marginal thickness in those membranes with the most defect-free microstructure. If research is continued in this area, emphasis should be placed on control, uniformity and reproducibility of the coating methodology. In addition, a final layer thickness of approximately 10 μm should be targeted, accomplished by multiple deposition cycles.

EXPERIMENTAL

The powder used for support fabrication ($SrCo_{0.8}Fe_{0.2}O_y$ and $SrCo_{0.5}$ FeO_x) was commercially obtained from Prax Air (Woodinville, WA). After some investigation into optimal fabrication conditions, supports were fabricated by uniaxial pressing of powder in a 0.5 in. die at 64 MPa, followed by sintering in air at 1050 ^oC (2 hr soak and 5 °C/min ramp rate). Sintering was conducted in a muffle furnace for air sintering, and in a tube furnace with continuous N_2 flow for N_2 sintering. The partially sintered supports were approximately 0.5 inch diameter disks that were strong but retained approximately 45% porosity. Though support sintering in N_2 was investigated, air sintering was adopted as the standard procedure because it produced less densification than N_2 sintering, and led to a microstructure that was more resistant to continued densification after membrane deposition. A series of experiments were also conducted utilizing a composite MgO/ $SrCo_{0.5}$ FeO_x support. For these supports, MgO powder (Ube, 0.2 μm mean particle size with some particles up to 1 μm) was mixed by mortar and pestle with varying amounts of $SrCo_{0.5}$ FeO_x powder prior to pressing and sintering. The support sintering procedure was the same as for the pure $SrCo_{0.5}$ FeO_x porous supports (2 hour soak at 1050 ^oC in air, with 5 ^oC/min ramp rates).

The ultrafine powder used to fabricate the ceramic membrane layers was synthesized using aerosol pyrolysis. A TSI 3076 aerosol generator was used with air or N_2 carrier/atomizing gas (35 psig, 1.5 slpm) to create an aerosol from an aqueous metal nitrate solution containing the metals in the desired ratio. The aerosol was carried through a three-zone Lindbergh furnace with 3 ft. heated length. The tube diameter (15 cm) provided a residence time of approximately 2.4 min. at 700 ^oC, which was the temperature adopted for the majority of powder syntheses. The powder was collected on a 142 mm diameter filter (cellulose acetate, 0.45 μm) after leaving the tube furnace (Fig. 1). Though both N_2 and air were investigated as carriers in powder synthesis, relatively little difference was found and air was the standard procedure for most of the membrane fabrication reported in this report.

Membrane layers were deposited by several methods, utilizing dilute slurries or more concentrated pastes made by various recipes. Table 1 summarizes the most important slurry/paste formulations that were explored, and the deposition method(s) used for each. Relatively dilute slurries (water or alcohol based) were deposited onto the porous substrates by spin coating and slip casting processes. For the slip-casting process, a dilute slurry was applied dropwise to the porous support. For the spin coating method, a thin layer of slurry was applied then spun using the spin coater (Headway), followed by reapplication. Both of these methods gave very thin layers requiring several layers of deposition. A doctor blade technique was used with thicker pastes that possessed a relatively high powder content (~20 to 50 wt%). With this technique, a fixed amount of the paste was spread uniformly across the surface of the support using a razor blade edge.

The spin coating procedure used for the multicomponent organic slurries (AS2 formulation in Table 1) was as follows. The dispersant (castor oil) and other organic additives were mixed with the aerosol powder, sonicated for 40 minutes, mineral spirit solvent was then added, followed by 60 minute sonication, then isopropanol and further additives, followed by another 60 minute sonication. This mixture was then coated by depositing one drop onto the center of a support that was mounted onto the spin coater chuck spinning at 2000 rpm. Spinning at 2000 rpm was

maintained for 40 s before spin down, when the sample was removed and subjected to a sintering cycle. Sintering treatments after each deposited membrane layer were similar to those used for the support. Air or nitrogen was used for the atmosphere (nitrogen for the organic paste/slurry formulations), with a ramp up/down rate of 5 °C/min and 1 hr soak at the maximum temperature.

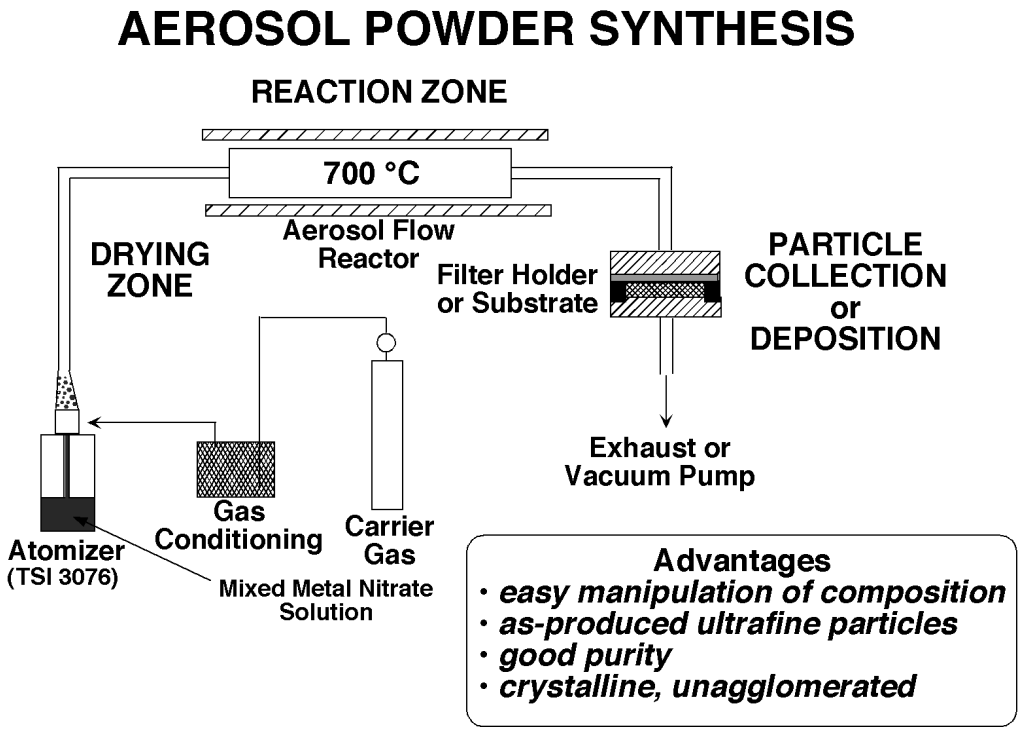

Fig 1. Aerosol pyrolysis process for producing submicron SCFO powder for membrane fabrication.

Table 1. Summary of paste and slurry formulations investigated. All amounts in weight percent.

ID	Powder	Solvent/Diluent	Dispersant	Binder	Plasticizer	Dep Method
PEG	~ 18	PEG-400: 82	-	-	-	Doctor blade
C2	42.9	MS: 18.3 IP: 9.1	CO: 19.4	PVB: 3.4	DBP: 2.3 PEG(300): 2.3 SA: 2.3	Doctor blade
AD2	32.3	MS: 18.9 IP: 9.4	CO: 28.9	PVB: 3.6	DBP: 2.3 PEG-300: 2.3 SA: 2.3	Doctor blade
AS2	18.3	MS: 35.7 IPl: 17.8	CO: 18.9	PVB: 3.1	DBP: 3.1 PEG-300: 3.1	Spin coating

PEG: polyethylene glycol (-molecular wt)
MS: mineral spirits
IP: isopropanol
CO: castor oil
PVB: polyvinyl butyral
DBP: dibutyl phthalate
SA: stearic acid

RESULTS AND DISCUSSION

Support Fabrication and Properties

Relatively early in the project densification studies on $SrCo_{0.5}FeO_x$ supports were completed in air and nitrogen. The results showed that comparable levels of densification are achieved at approximately 50 ^oC lower in nitrogen than in air (Fig. 2). It was found that reasonably strong porous supports could be fabricated at approximately 1050 ^oC while retaining close to 45% porosity in the supports. The microstructure is very different for air and N_2 sintering. With air sintering, large plate-shaped grains are formed, whereas grains remain more equiaxed with N_2 sintering (Fig. 3). The crystalline phase content in sintered supports also depended on the sintering atmosphere, with air sintering leading to the desired (i.e., high oxygen permeability) layered perovskite structure, and N_2 sintering leading to a mixture of several phases

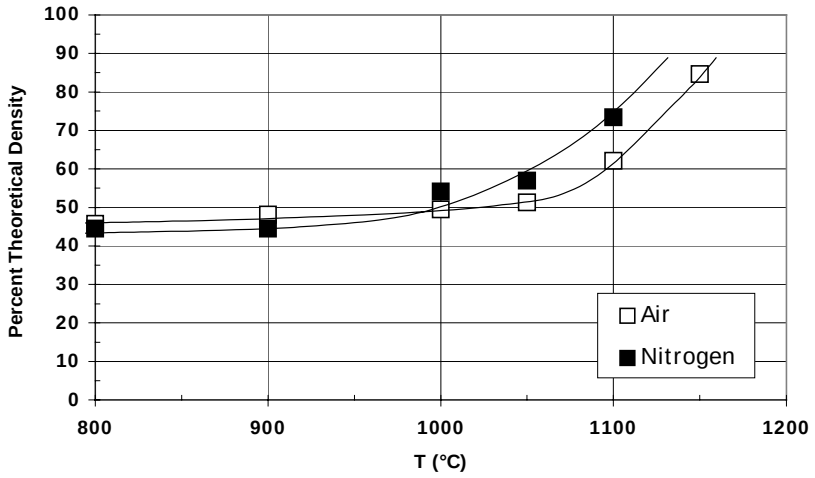

Fig. 2. Densification of $SrCo_{0.5}FeO_x$ supports as a function of sintering temperature and atmosphere.

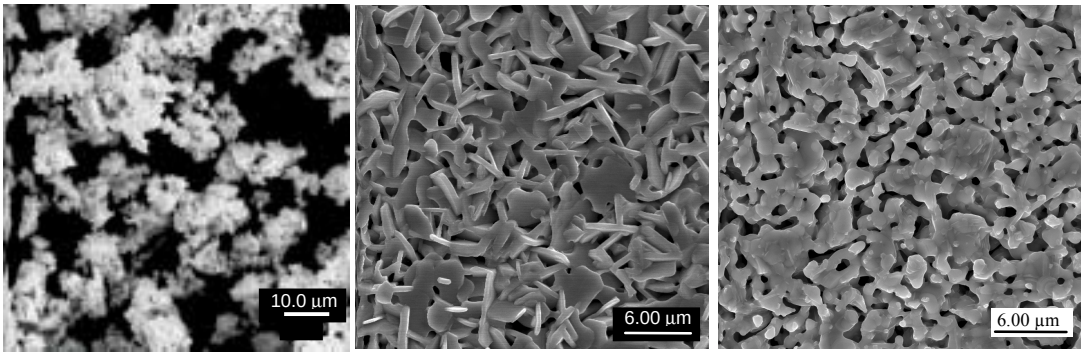

As-received commercial powder **Air at 1050 °C** **N_2 at 1050 °C**

Fig. 3. Scanning electron micrographs showing SrCo0.5FeOx supports after sintering at 1050 °C in air and nitrogen.

(brownmillerite, CoO, and layered perovskite) (Fig. 4). Based on these results, the standard sintering procedure for supports was adopted as sintering at 1050 ^{o}C in air for 2 hr with ramp rate of 5 ^{o}C/min.

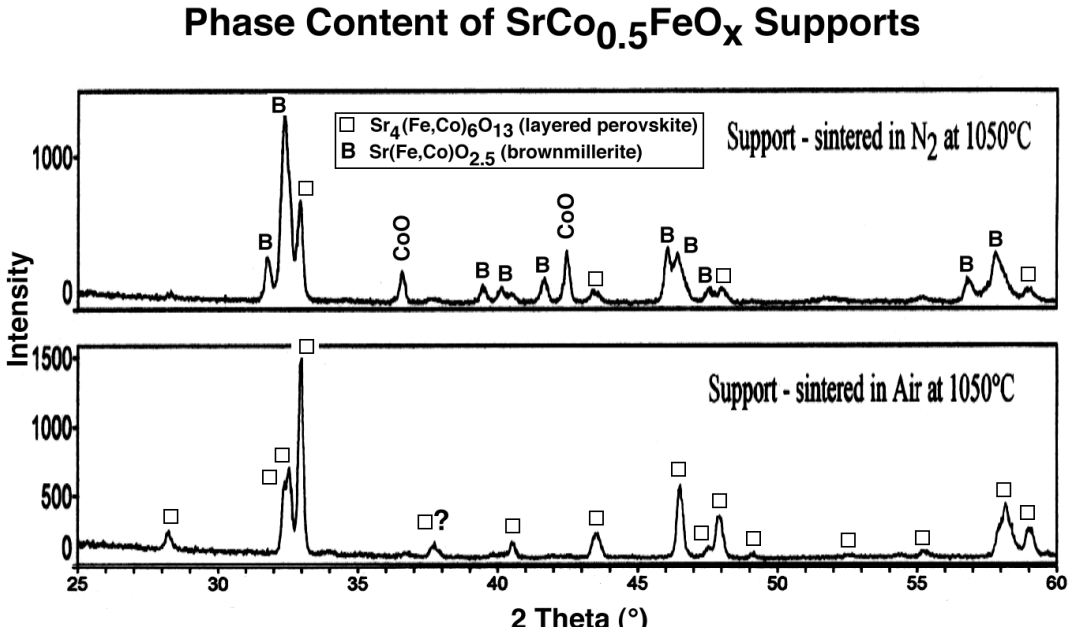

Fig. 4. X-ray diffraction data for $SrCo_{0.5}FeO_x$ supports after sintering in air and nitrogen at 1050 °C.

One strategy that was explored to reduce cracking in sintered supported membranes was to reduce the sinterability of the supports by using a composite powder, thus enabling us to sinter the supported films at a temperature very near the SCFO melting point. The reasoning was that if the films are more liquid-like, then they should be able to flow in response to stress, rather than be forced to crack or delaminate from the support. However, sintering near the SCFO melting point would also densify the underlying support if some strategy is not employed to inhibit support sintering, a fact which we confirmed by experiment. We attempted to inhibit support sintering by mixing MgO powder with the SCFO support powder prior to support sintering. MgO has a very high melting point (2852 ^{o}C), and should sinter minimally at the melting temperature of the SCFO phases, which is around 1200 ^{o}C. In addition, MgO has been found to be chemically nonreactive with the SCFO phases.[3] Thus, the effect of adding varying amounts of MgO to the support was investigated. The addition of 40 wt% MgO to the support served to inhibit densification of the support at 1200 ^{o}C where film and support would have been fully sintered and indistinguishable in the absence of the MgO (Fig. 5). With MgO added to the support, film sintering was conducted at temperatures as high as 1400 ^{o}C. At sintering temperatures of 1200 and 1300 ^{o}C the support densification appears inhibited and the film remains clearly distinct from the support (Fig. 5). However, although the film shows rounding of featurse indicative of partial melting, it retains what appears to be an open network structure. This may indicate that complete melting does not occur, or that wetting of the porous support below somehow prevents the formation of a contiguous film. This strategy demonstrated

inhibited sintering of the support, but we were unable to achieve continuous dense membrane layers for reasons that were not fully understood.

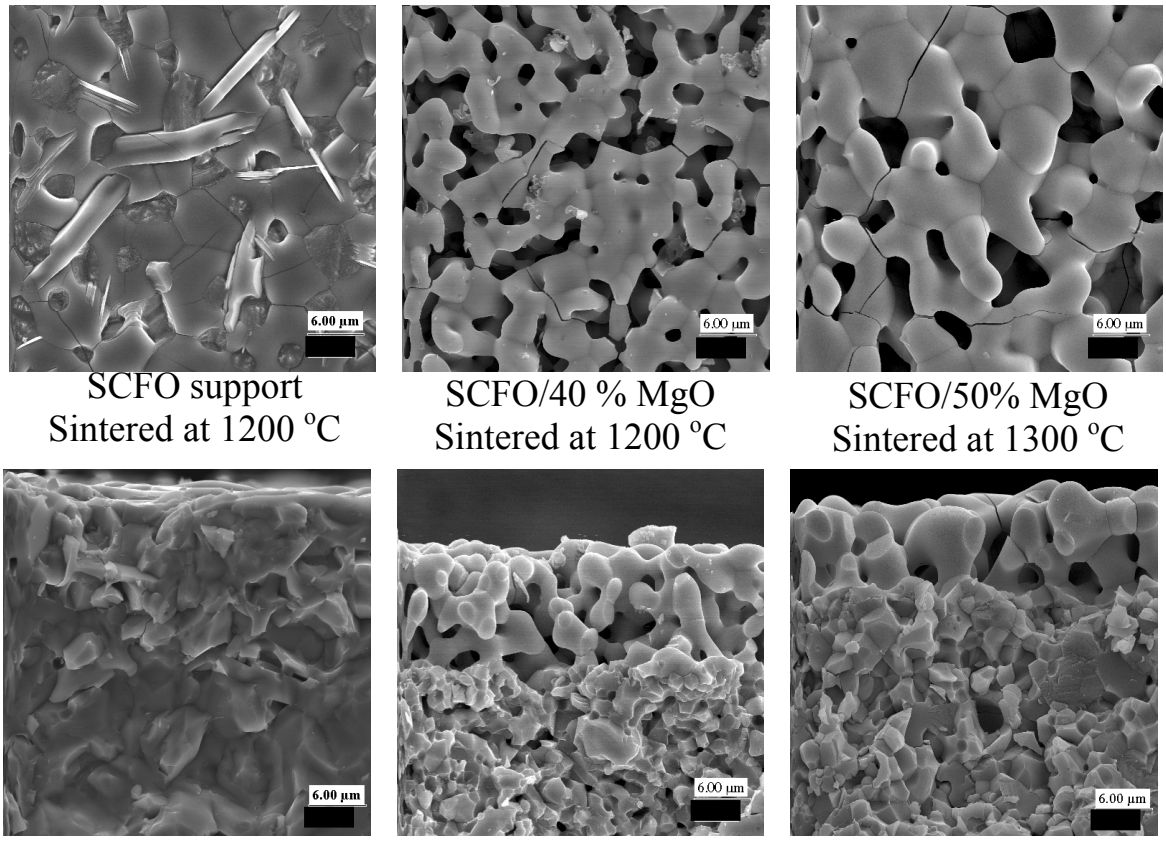

Fig. 5. Sintering of $SrCo_{0.5}FeOx$ films on composite MgO/SCFO supports compared to sintering on a pure SCFO support.

Aerosol Powder Synthesis

The aerosol-derived powders produced at 700 °C in either air or nitrogen were submicron, with particle sizes ranging from roughly 0.1 to 0.5 µm (Fig. 6). The powder was essentially single phase perovskite $Sr(Co,Fe)O_{3-x}$ as-produced (Fig.7). It was somewhat surprising that the layered perovskite or brownmillerite phases that were seen with sintering of the SCFO supports did not appear in the as-produced powders, especially since the overall composition of the powders is not consistent with single phase $S(Co,Fe)O_{3-x}$. This indicates that the simple perovskite structure is kinetically preferred, and that the reactor residence time is sufficient to develop crystalline perovskite but not sufficient to allow the layered structures to evolve.

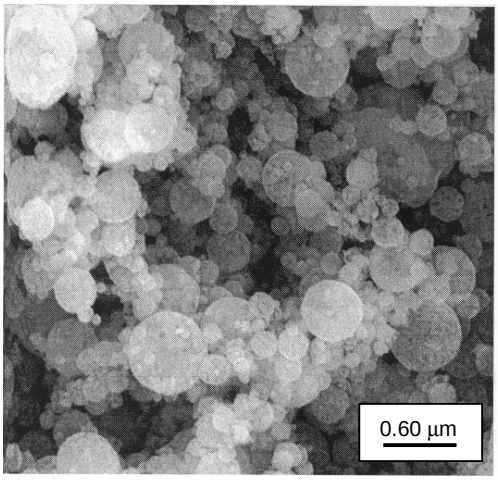

Fig. 6. Scanning electron micrograph of $SrCo_{0.5}FeO_x$ powder produced by aerosol pyrolysis at 700 °C.

Membrane Layer Deposition and Sintering

While other deposition methods were explored, the most important results were obtained using three deposition methods: (1) doctor blade deposition of PEG paste, (2) doctor blade deposition of multicomponent organic paste, and (3) spin coating of multicomponent organic slurry. High levels of densification and determination of crystalline phase behavior were accomplished with the PEG pastes. However, cracking was severe. The use of a more complex paste formula involving organic dispersant, binders, and plasticizers provided a large reduction in cracking, but did not eliminate it. The most successful deposition method from the standpoint of cracking was the use of spin coating of multiple layers of a relatively dilute slurry of powder in the presence of organic dispersant, binders, and plasticizers. This approach led to crack free films, but never yielded defect-free ("gas-tight") membranes. The most important results from each of these deposition approaches are summarized below.

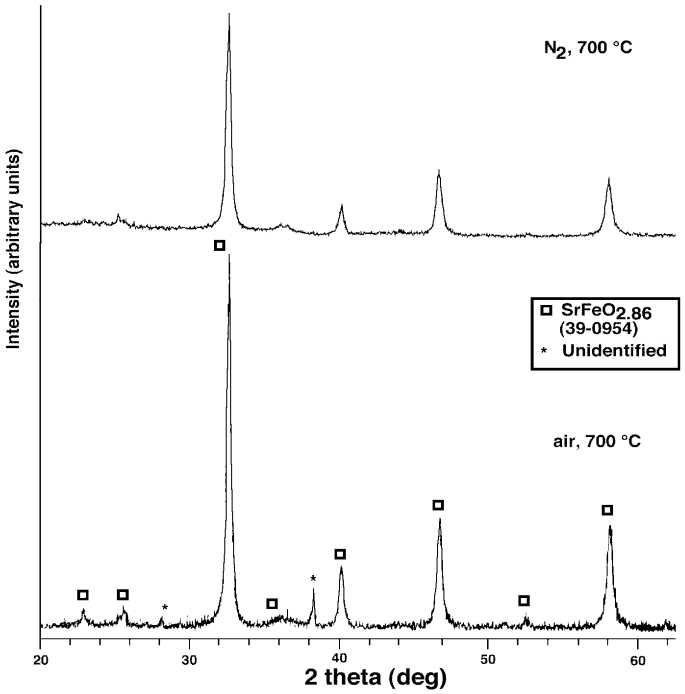

Fig. 7. X-Ray diffraction result for $SrCo_{0.5}FeO_x$ powders made by aerosol pyrolysis using air and N_2 as carrier gas.

Doctor Blade Deposition of PEG Pastes

The application of a single layer of the paste by the manual doctor blade method led to a layer that was typically 20-30 μm thick before sintering and uncracked. After calcination in air at 800 °C, some particle–particle necking was evident; however, relatively little shrinkage appeared to have occurred (Fig. 8). This is consistent with the shrinkage (densification) profiles determined for the SCFO supports (Fig 2). There is little or no cracking evident in films calcined at 800 °C, and the cross-sectional micrograph shows that there is still high porosity in the film.

Quantitative evaluation of the film densification/shrinkage was not done as a function of temperature, however SEM images reveal that significant sintering occurs for temperatures above 900 in air or N_2 (Figs. 9 and 10). Relatively little densification occurred in the pre-sintered supports at this temperature, which shows the enhanced sintering of the ultrafine aerosol powder. It is also interesting that pronounced growth of plate-shaped grains begins to occur at approximately 900 ^oC for air sintering (Fig. 10). We have determined that these plate-shaped grains are characteristic of the layered perovskite stucture. Thus 900 ^oC is the

approximate temperature where the perovskite structure begins to form the layered structures in air over the time scales of our sintering experiments.

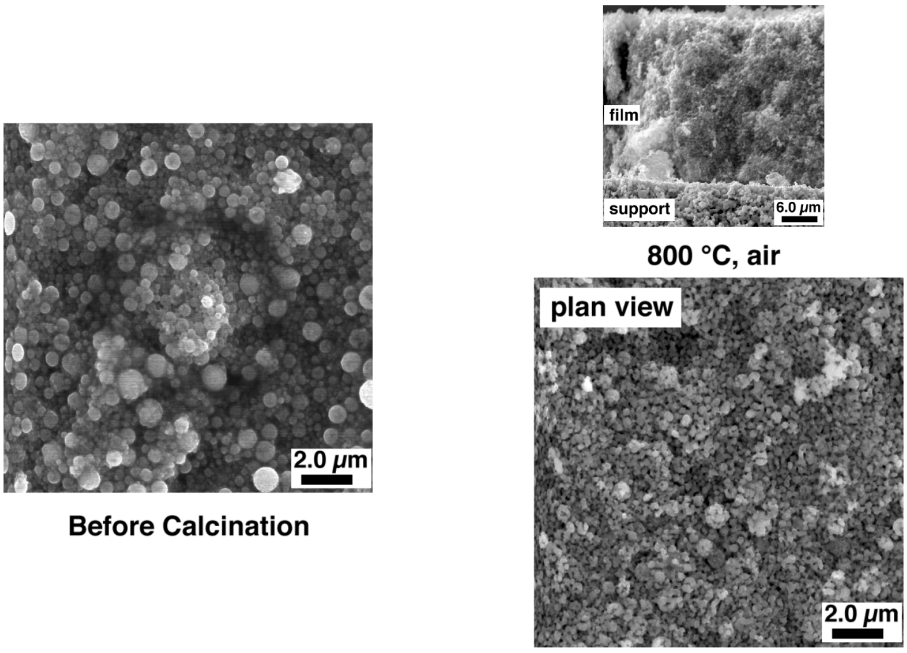

Fig. 8. Scanning electron micrographs of $SrCo_{0.5}FeO_x$ films after application of PEG paste ("before calcination"), and after calcining at 800 ^oC in air.

With the use of higher sintering temperatures, the areas of film continued to densify, displaying microstructures that depended on atmosphere in much the same way that was seen with the supports (i.e. plate shaped grains in air and equiaxed grains in N_2). Furthermore, N_2-sintered film material became fully dense (by SEM observation) at a sintering temperature of approximately 1050 ^oC, whereas the air-sintered films were not dense at that temperature (see Figs. 9 and 10). However, in both cases pronounced cracking had occurred during densification, leading to the large areas of open underlying support that can be seen in the lower magnification images in Fig. 11. It is noteworthy that the film material can be densified completely without densifying the underlying support, which is one of the major objectives in the project; however, the uncovered support areas prevent the supported film from being functional as a membrane.

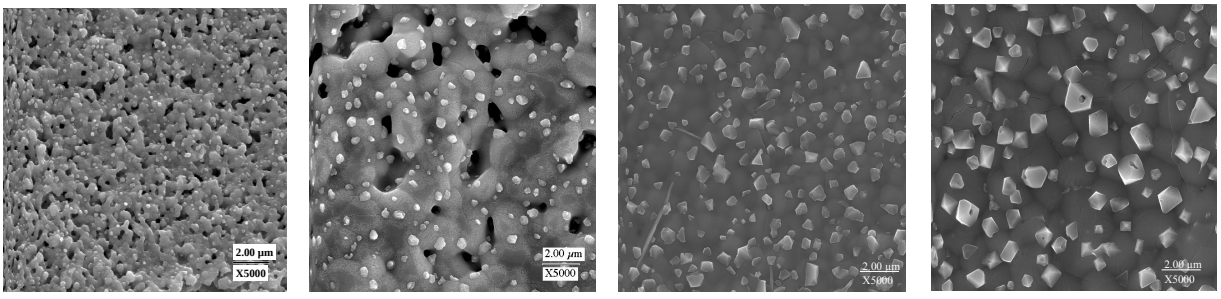

Fig. 9. Scanning electron micrographs of $SrCo_{0.5}FeO_x$ films sintered in N_2 at several temperatures.

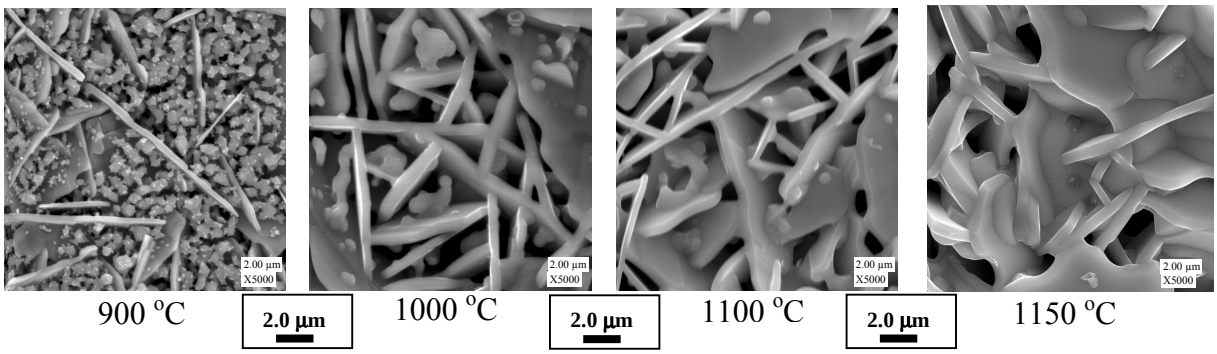

Fig. 10. Scanning electron micrographs of $SrCo_{0.5}FeO_x$ films sintered in air at several temperatures.

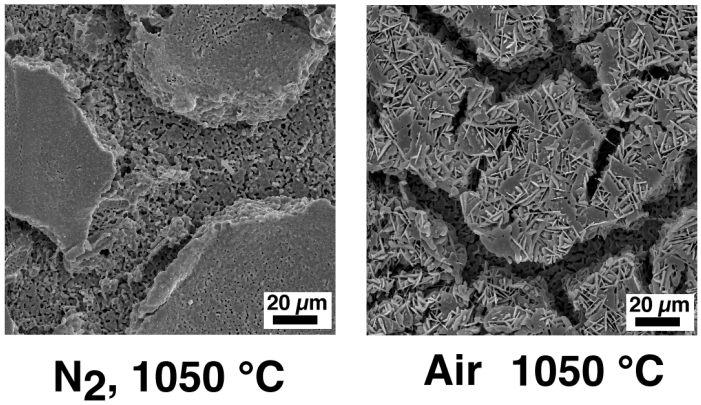

Fig. 11. Relatively low magnification scanning electron micrographs of $SrCo_{0.5}FeO_x$ films sintered in N_2 and air at 1050 °C.

The crystalline phase evolution of the films that occurred with sintering was also investigated to a limited extent. Using grazing angle XRD, the XRD pattern of a film sintered in N_2 at 1050 °C is shown in Fig. 12. This shows that the film is a mixture of layered perovskite and CoO, possibly also containing some of the cubic perovskite since its peaks overlap with the layered perovskite. This multiphase mixture is consistent with literature reports for this composition,[10,11] although it is not consistent with our results for supports sintered in N_2, which displayed a composite mixture of phases consisting primarily of the brownmillerite phase, but without the layered perovskite. In this case, the support had been pre-sintered in air and was in the layered perovskite phase before membrane deposition. It is interesting and fortuitous that, after conducting the film sintering in N_2, the phase content remained as layered perovskite rather than converting to brownmillerite.

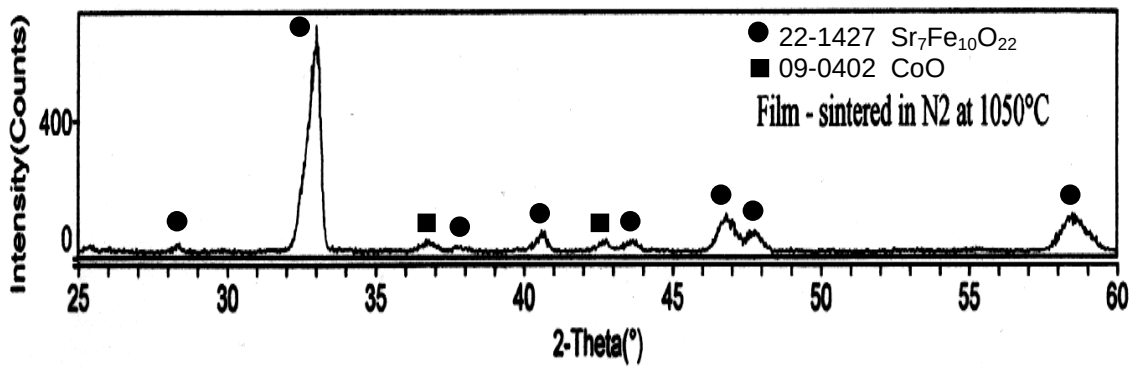

Fig. 12. Glancing-angle x-ray diffraction of supported $SrCo_{0.5}FeO_x$ thick film after sintering in N_2 at 1050 °C.

Doctor Blade Deposition of Multicomponent Organic Paste

To make progress on the elimination of cracking in the paste-derived membrane layers, paste and ink formulations that have been used for screen printing and tape casting of ceramic films were reviewed.[16,17] Paste formulations based on organic vehicles can have advantages over aqueous vehicles due to good solubility of organic additives, as well as lower inherent surface tension, which effects stress development during drying. An organic formulation was developed based on a mixture (2:1) of mineral spirits and ispropanol, incorporating castor oil as dispersant, polyvinyl butyral as binder, and a mixture of dibutyl phthalate, polyethylene glycol (MW 300) and stearic acid as plasticizers. The ratios of the various components were varied somewhat, and the formulas for the results presented here were tabulated in the Experimental section. Typically, we kept the additive ratios fixed, and varied the ratio of solvent and powder to get an appropriate viscosity paste for spreading. Appropriate viscosity was based on experience and qualitative judgment, and was not measured quantitatively.

Pastes were deposited by spreading of the paste using a hand-held single-edged razor. While some exploration of air sintering was done, we found that N_2 sintering of supported membranes using supports that had been partially pre-sintered in air gave the best results. We attribute this to the accelerated sintering generally observed using N_2. By pre-sintering the supports in air, a relatively stable porous microstructure is provided that sinters significantly slower in subsequent processing than the aerosol powder-derived membrane layer. The ultrafine particle size of the aerosol powder is also an important factor in the enhanced sintering of the membrane layer relative to the underlying chemically identical support. Fig. 13 shows plan and cross-sectional views of the membrane top surface for single-layer membranes prepared by doctor blade deposition using paste formulation AD2 (see Table 1). At the scale shown in Fig. 13, densification of the top surface appears almost complete after sintering at 1100 °C. Cross-section of a fracture surface (Fig. 13 (c)) shows a membrane thickness of approximately 10 μm, and confirms the essentially complete densification of the top layer as well as the remaining presence of porosity in the underlying support. However, the cross-sectional view, taken at a downward angle, also shows evidence of cracks and irregularities in the membrane surface not apparent in the SEM plan view. While cracking was dramatically reduced in these membranes compared to those produced by the simple PEG-based pastes, coverage and defects were still significant enough to limit the overall gas-tightness of the membrane (see permeation section).

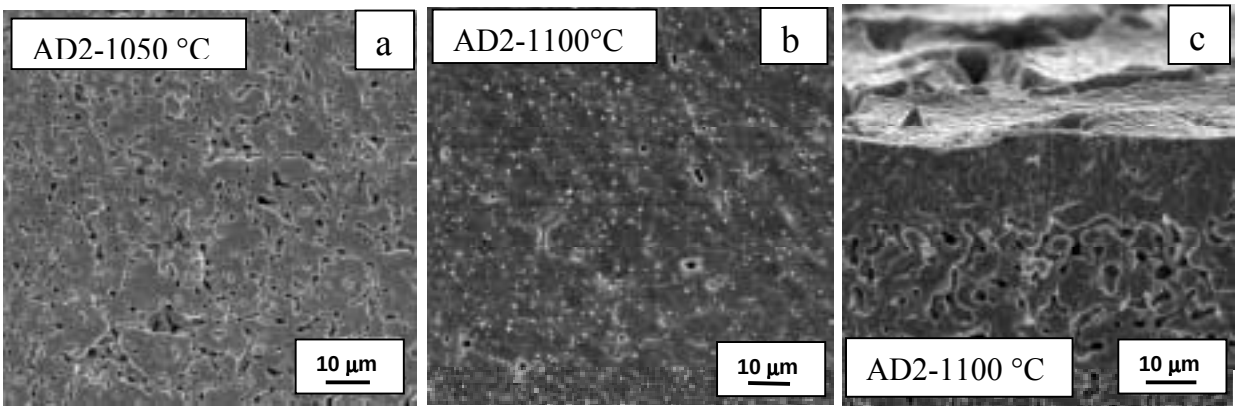

Fig. 13. Scanning electron micrographs showing plan views of membrane top surfaces after doctor blade deposition of single layer and sintering in nitrogen at 1050 °C (a) and 1100 °C (b); and cross-sectional view (fracture surface) of membrane and underlying support after sintering at 1100 °C in nitrogen.

Spin Coating of Multicomponent Organic Slurry

As a means to obtain better control of membrane layer thickness, we explored the use of spin coating using a similar, but more dilute, formulation to that used for the doctor-blade results presented in the previous section. For these slurries the overall powder content was roughly half that used for the doctor blade deposition (see Table 1). In addition, no stearic acid was used which also helped to reduce viscosity of the slurry. Successive layers were deposited by this procedure, with each successive layer sintered in N_2 at 1100 °C. Because these membranes conduct electrons well, we were able to conduct SEM on the membranes after each layer without any sort of conductive coating, before depositing an additional layer, thus tracking the elimination of defects with each layer. Simultaneously, we subjected an uncoated support to the same sintering cycles to record the changes in support microstructure. Fig. 14 shows the micrographs for this series of depositions and sintering cycles. There is a dramatic increase in pore coverage with the deposition of a second layer, with no apparent open pores evident after the second layer. The support undergoes noticeable densification after the first sintering cycle, but appears to be relatively stable after that. Cross-sectional SEM views (Fig. 15) after one coating and four coats, show no apparent surface layer after one coat but a clear layer about 6 µm thick after four coats. The fracture surface view (Fig. 15 (c)) shows substantial open porosity in the support after four sintering cycles. Permeation measurements presented in the next section bear this out.

The plan views depicted in Fig. 14 were representative of essentially the entire membrane surface for these spin-coated membranes, except very near the outer edges. There was no cracking apparent in the sintered membrane layers, in contrast to all other deposition procedures that were used during this project. Thus, this deposition procedure was the most successful approach developed during the project with respect to controlling cracking in the membrane layer. Low-temperature permeation measurements, discussed in the next section, revealed that these membrane still contained significant defects.

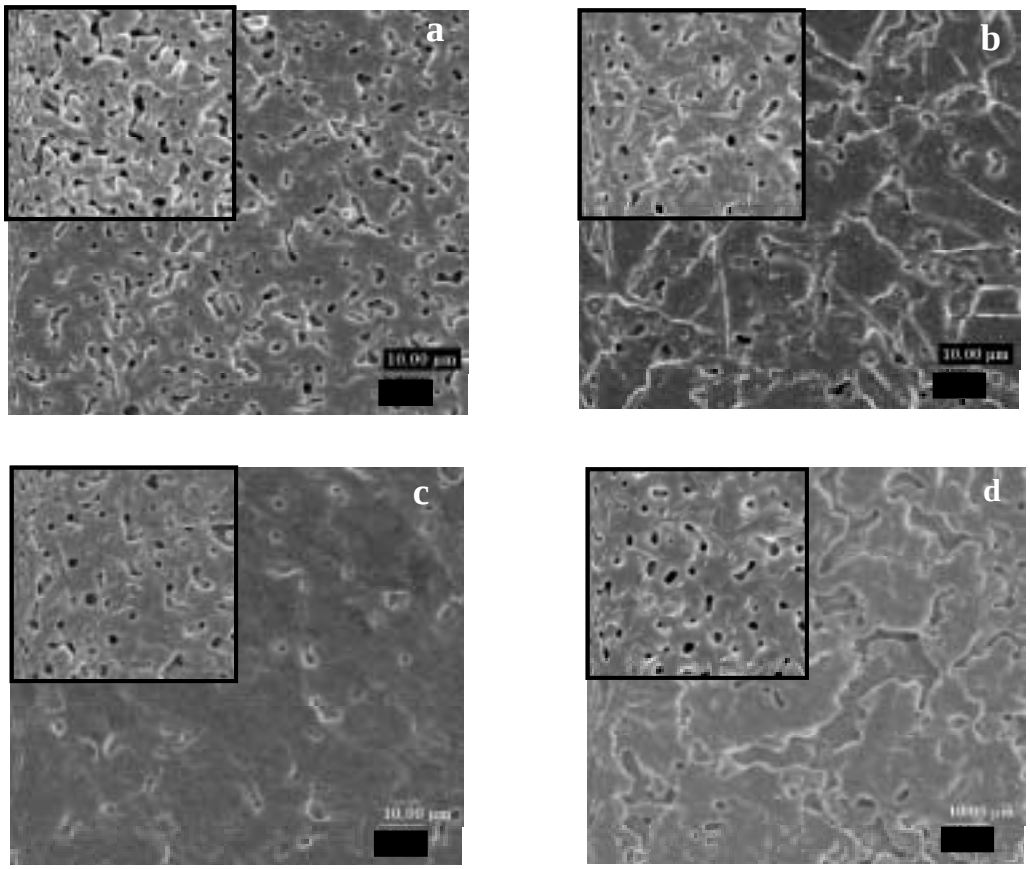

Fig. 14. SEM plan-views of surface of membranes deposited by spin coating of AS2 slurry formulation with one (a), two (b), three (c) and four (d) coats. After each coating the membrane was sintered in N_2 at 1100 °C. The insets show the microstructure of the porous support (same magnification) after undergoing the same sintering cycles.

Permeation Characteristics of Supported Membranes

Because of the extensive cracking in the membrane layers produced in the earlier years of the project, few permeation measurements were conducted. However, systematic permeation measurements (i.e., low temperature, pressure-driven leakage measurements) were conducted with the doctor blade and spin-coating deposition procedures using the multicomponent organic pastes and slurries (AS and AD formulations in Table 1). In permeation testing of supported membranes, the measured permeation may reflect resistance coming from both the support and membrane layer. Thus, it is necessary to separately measure or estimate the permeability (or resistance) from the support, which allows the permeability/resistance of the membrane layer itself to be calculated. For our spin-coating deposition, multiple coats were applied with sintering between each coat. We conducted parallel sintering treatments of a support to enable us to properly account for the support resistance. The low temperature permeation measurements were conducted with N_2 utilizing a relatively small pressure difference. This measured the pressure-driven leakage through the supported membrane by viscous and/or Knudsen flow. No other permeation gases were used because the only goal of these measurements was to determine if membrane layers were sufficiently defect free to merit high

temperature oxygen permeation measurements. Unfortunately, no membranes produce in this project achieved this.

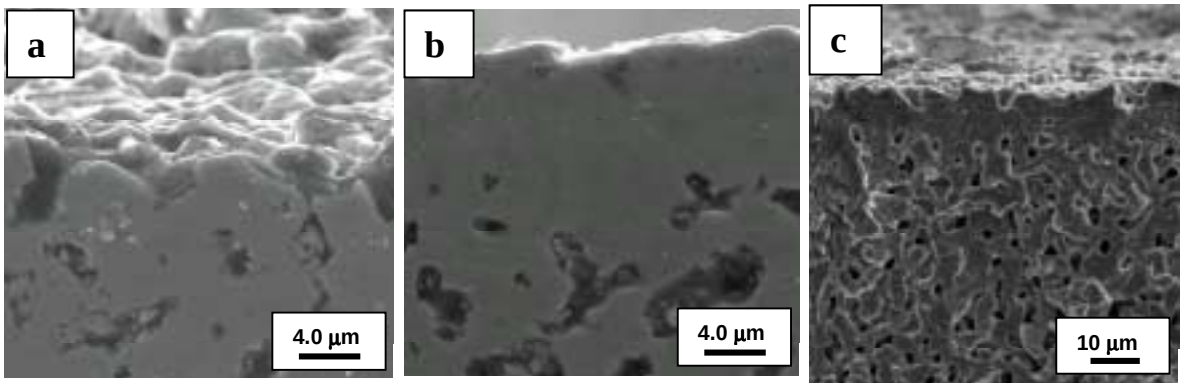

Fig. 15. SEM cross-sectional views of spin-coated membrane layers and underlying porous support: (a) polished surface after one coat, (b) polished cross section after four successive coats with sintering, and (c) fracture surface after four coats with sintering.

Permeability measurement results on one doctor blade membrane (single coat, AD2 formulation), a sequence of four spin-coated membrane layers, and the supports after undergoing sequential sintering treatments are presented in Fig. 16. Permeability values are tabulated in Table 2. The overall permeability (F_T) of a supported membrane is calculated from measured data by the following equation:

$$F_T = \frac{J}{\Delta P}, \tag{1}$$

where J is the measured permeation flux, and ΔP is the overall pressure difference across the membrane. If the permeability of the support (F_S) is measured or known separately, the permeability of the membrane layer (or layers) itself (F_M) can determined from the following equation:

$$\frac{1}{F_M} = \frac{1}{F_T} - \frac{1}{F_S} \tag{2}$$

For the membrane deposited by doctor blade deposition, the permeability was essentially unchanged by the addition of the membrane layer. This indicates that the defects were large enough that the resistance of the membrane layer was not significant relative to that of the support. For the spin coating deposition, it is apparent from the graphical data depiction that a relatively small decrease in permeability with the first coating leads to a much larger decrease with the second coating, and relatively small decreases occur with subsequent coats. This is consistent with the appearance in plan-view SEM (Fig. 14). The supports undergo a progressive, but relatively slow, decrease of permeability with the sequential sintering cycles associated with multiple spin coating deposition and sintering. Membrane permeability values calculated using eq. (2) are listed in Table 2. These values clearly show a large drop in permeability with the second spin-coated layer, with smaller but progressive decreases after that.

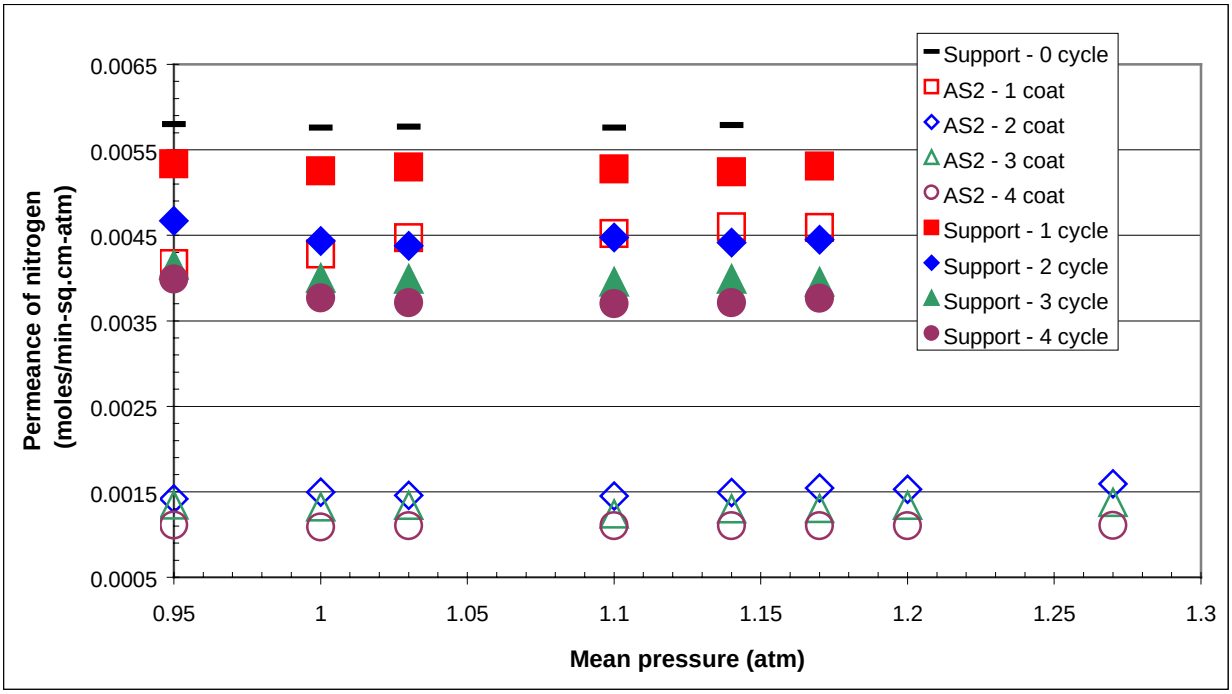

Fig. 16. Room temperature nitrogen permeability measurements on supports and supported membranes prepared by spin coating deposition.

Table 2. Measured permeability values for supports (F_S), supported membranes (F_T) and membrane layer (F_M) deposited by doctor blade and spin-coating deposition.

SUPPORT	F_S (mol/min-cm^2-atm)	SUPPORT + MEMBRANE	F_T (mol/min-cm^2-atm)	F_M (mol/min-cm^2-atm)
S0: support (0 cycles)	0.0058	Uncoated Support		
S1: support after 1 cycle	0.0052	AD2: Doctor Blade – 1 layer	0.0058	large
S1: support after 1 cycle	0.0052	AS2-1: Spin Coating – 1 coat	0.0046	0.040
S2: support after 2 cycles	0.0044	AS2-2: 2 coats	0.00147	0.0022
S3: support after 3 cycles	0.0040	AS2-3: 3 coats	0.0013	0.0019
S4: support after 4 cycles	0.0037	AS2-4: 4 coats	0.0011	0.0016

MOCVD Defect Mending

Metal organic chemical vapor deposition (MOCVD) was explored as a technique for mending defects in SCFO membranes. The idea, briefly, was to conduct an MOCVD reaction within defects of a membrane such that the defects would be blocked by a chemically compatible material. The strategy was to use a reaction that required a co-reactant (such as H_2 or O_2) in

addition to the metal organic precursor, and to control contact of the reactants using counter-directional convection or diffusion such that deposition only occurs in the pores or defects. A metal organic precursor, $Fe(tmhd)_3$ (tmhd=tetramethylheptanedionate), was flowed past the membrane layer side of a defective SCFO membrane, while a O_2-containing gas was flowed past the opposite (support) side of the membrane. It had been demonstrated that $Fe(tmhd)_3$) could be sublimed readily at 200 ^oC using a N_2 carrier gas, and would react to produce iron oxide at 280 – 300 ^oC in the presence of O_2, while remaining stable to well over 300 ^oC in the absence of oxygen. Experiments were conducted at varying the pressure difference across the membrane to get an appropriate balance between transport of precursor/carrier and oxygen so that deposition occurs in the region of the membrane layer. Using this approach, we were able to obtain iron oxide deposition on the membrane surface, but were unable to obtain sufficiently controlled deposition to significantly mend membrane defects.

CONCLUSION

One of the main premises for this project as originally proposed was that a supported membrane layer made of ultrafine powder could be sintered without simultaneously densifying the underlying support. Using aerosol-derived $SrCo_{0.5}FeO_x$ powder with mean particle size below 0.5 μm, we demonstrated that the membrane layer could indeed be sintered to high density without densifying the chemically identical underlying support. The supports were fabricated with a coarser powder, and presintered in air to produce a microstructure that was comparatively stable to further sintering, while the ultrafine particle size of the aerosol powder sintered rapidly. Sintering atmosphere was also shown to be an important variable, and preferential sintering of the membrane layer was also promoted by sintering in N_2, after presintering the supports in air. Cracking of the supported membrane layer during drying and the removal of the liquid vehicle in the early stages of sintering was a major problem throughout the project. Cracking was finally eliminated by utilizing an organic paste/slurry formulation that was similar to formulations that have been reported for ceramic tape casting. The most successful formulations utilized castor oil as a dispersant, polyvinyl butyral as a binder, and dibutyl phthalate and polyethylene glycol as plasticizer, with the solvent (mineral spirits/isopropanol) amount controlled to give appropriate viscosity for doctor blading or spin coating. With these formulations, cracking in the membrane layer as detected by SEM observation was essentially eliminated in thin membrane layers deposited by spin coating. However, room-temperature permeation measurements with nitrogen revealed that the membranes were not sufficiently defect free for high temperature testing.

The use of the non-aqueous paste/slurry formulations essentially eliminated crack and major issues associated with large scale defects in the membrane layer. We believe that the factors that prevented the achievement of defect free membranes may be associated with the (lack of) uniformity of the layers from edge-to-edge of the support, and marginal thickness. It appears from our experiments that overall thickness of 10 μm may be desirable, accomplished in 3 to 5 separately deposited layers. More systematic evaluation of slurry viscosity would be valuable, and a carefully designed doctor blade system could ultimately be better than spin coating, which has significant practical limitations for anything by small supports.

REFERENCES

1. B. C. H. Steele, "Oxygen Ion Conductors and their Technological Applications", Mater. Sci. Eng. **B13**, 79 (1992).
2. T. L. Ward, G. P. Hagen, and C. Udovich, "Assessment of Inorganic Membrane Technology of Petrochemical Applications", in *Proceedings of the Third International Conference on Inorganic Membranes*, July 10-14, 1994, Worcester Polytechnic Institute, 100 Institute Rd, Worcester, MA 01609.
3. R.W.Schwartz, J.P. Collins, M.F. Ng, C.J. Brinker, T.L. Ward, R.Sehgal, C. Xia, C.A. Udovich, J. Masin, and G.P. Hagen, "Inorganic Membrane Reactor Technology CRADA #1176: Final Report and Assessment of Membrane Technology, Sandia Report SAND97-0949 (1997).
4. U. Balachandran, J.T. Dusek, R. L. Mieville, R. B. Poeppel, M. S. Kleefisch, S. Pei, T. P. Kobylinski, C. A. Udovich and A.C. Bose, "Dense Ceramic Membranes for Partial Oxidation of Methane to Syngas", Appl. Catal. A **133**, 19 (1995).
5. Y. Teraoka, T. Fukuda, N. Miura, and N. Yamazoe, "Development of Oxygen Semipermeable Membrane Using Mixed Conductive Perovskite-Type Oxides (Part 2) - Preparation of Dense Film of Perovskite Type Oxide on Porous Substrate", J. Ceram. Soc. Jpn. Inter. Ed. **97**, 523 (1989).
6. Y. Teraoka, H.-M. Zhang, S. Furukawa and N. Yamazoe, "Oxygen Permeation Through Perovskite-Type Oxides", Chem. Lett. **1985**, 1743-1746 (1985).
7. Y. Teraoka, T. Nobunaga and N. Yamazoe, "Effect of Cation Substitution on the Oxygen Semipermeability of Perovskite-type Oxides", Chem. Lett. **1988**, 503 (1988).
8. Y. Teraoka, H. M. Zhang, K. Okamoto and N. Yamazoe, "Mixed Ionic-Electronic Conductivity of $La_{1-x}Sr_xCo_{1-y}Fe_yO_{3-\delta}$ Perovskite-Type Oxides", Mat. Res. Bull. **23**, 51 (1988).
9. B. Ma, U. Balachandran, J.-H. Park and C. U. Segre, "Electrical Transport Properties and Defect Structure of $SrFeCo_{0.5}O_x$", J. Electrochem. Soc. **143** (5), 1736 (1996).
10. S. Guggilla and A. Manthiram, "Crystal Chemical Characterization of the Mixed Conductor $Sr(Fe,Co)_{1.5}O_y$ Exhibiting Unusually High Oxygen Permeability", J. Electrochem. Soc. **144** (5), L120 (1997).
11. B.Ma, J. P. Hodges, J. D. Jorgensen, D. J. Miller, J. W. Richardson, Jr., and U. Balachandran, "Structure and Property Relationships in Mixed-Conducting $Sr_4(Fe_{1-x}Co_x)_6O_{13\pm y}$", J. Solid State Chem. **141**, 576-586 (1998).
12. A. Gurav, T. Kodas, T. Pluym and Y. Xiong, "Aerosol Processing of Materials", Aerosol Sci. Technol. **19**, 411 (1993).
13. T. T. Kodas and M. Hampden-Smith, *Aerosol Processing of Materials*, Wiley-VCH, New York (1999).
14. Armstrong, S. Gugilla, and A. Manthiram, "Oxygen permeation studies of $Sr_4Fe_{6-x}Co_xO_{13+\delta}$", Mat. Res. Bull. **34**(6), 837 (1999).
15. H. Fjellvag, B.C. Hauback, and R. Bredsen, "Crystal structure of the mixed conductor $Sr_4Fe_4Co_2O_{13}$", J. Mater. Chem. **7**(12), 53 (1997).
16. D. J. Shanefield, *Organic Additives and Ceramic Processing, Second Edition: with Applications in Powder Metallurgy, Ink and Paint*, Kluwer, Boston (1996).
17. J.S. Reed, *Principles of Ceramic Processing*, Wiley Interscience, New York (1995).